Sonochemical Synthesis and Characterization of Nanometer-Size Transition Metal Oxides from Metal Acetates

R. Vijaya Kumar, Y. Diamant, and A. Gedanken*

Department of Chemistry, Bar-Ilan University, Ramat-Gan 52900, Israel

Received February 23, 2000. Revised Manuscript Received May 25, 2000

Transition metal oxide nanoparticles have been synthesized sonochemically from metal acetates. The metal oxide nanoparticles are characterized using X-ray diffraction (XRD), diffuse reflection spectroscopy (DRS), transmission electron microscopy (TEM), and BET nitrogen adsorption. The results of DRS are analyzed in detail, and the band gap energies for CuO, ZnO, and Co_3O_4 are seen to be 2.18, 3.35, and 2.26 (3.40), respectively. Different particle sizes, morphology, and yields are observed when water and 10% water−*N*,*N*-dimethylformamide (DMF) are used as solvents, and the possible mechanisms are discussed.

Introduction

Metal acetates are useful reagents, particularly in organic synthesis and in the preparation of some industrially important metal and metal oxide catalysts. Nanometer-sized metals, semiconductors, and oxides are of greatest interest because they can have physical and chemical properties that are not characteristic of the atoms or of the bulk counterparts. The large ratio of surface area to volume can contribute to some of the unique properties of nanoparticles.[1−5] The oxides of transition metals (TM) such as iron, nickel, cobalt, copper, and zinc have many important applications, including magnetic storage media, solar energy transformation, electronics, semiconductor, varistor, and catalysis.[6−19] In the past, some successful attempts have been made to synthesize the nanoparticles of metal oxides[20−24] by chemical methods. Recently, sonochemical processing has been proven as a useful technique for generating novel materials with unusual properties. Sonochemistry arises from acoustic cavitation phenomenon, that is, the formation, growth and implosive collapse of bubbles in a liquid medium.[25] The extremely high temperatures (>5000 K) and pressure (>20 Mpa) and very high cooling rates ($>10^7$ K s^{-1})[26] attained during acoustic cavitation lead to many unique properties in the irradiated solution. Using these extreme conditions, Suslick and co-workers have prepared amorphous iron[26] by the sonochemical decomposition of metal carbonyls in an alkane solvent. Recently, we have successfully prepared nanoparticles of chromium, manganese, molybdenum, europium, terbium oxides, and gallium oxide hydroxide[27−30] sonochemically. The as-prepared materials were fabricated either in the amorphous state or in the crystalline phase. In the present investigation, we report on the general sonochemical synthesis of metal oxides from metal acetates.

Experimental Section

The synthesis of metal oxide nanoparticles has been carried out as follows: 500 mg of zinc(II) acetate dihydrate (Aldrich 98+%), copper(II) acetate monohydrate (Aldrich 98+%), cobalt(II) acetate (Aldrich 99.9%), or iron(II) acetate (Aldrich 95%)

* Corresponding author. E-mail: gedanken@mail.biu.ac.il. Fax: +972-3-5351250.

(1) Morse, M. D. *Chem. Rev.* **1986**, *86*, 1049.
(2) Halperin, W. P. *Rev. Mod. Phys.* **1986**, *58*, 533.
(3) Henglein, A. *Chem. Rev.* **1989**, *89*, 1861.
(4) Stucky, G. D.; MacDougall, J. E. *Science* **1990**, *247*, 669.
(5) Kresin, V. V. *Phys. Rep.* **1992**, *220*, 1.
(6) Livage, J. *J. Phys. Colloq.* **1981**, *42*, 981.
(7) *Ferromagnetic Materials*; Wohlfarth, E. P., Ed.; North-Holland: Amsterdam, New York, Oxford, Tokyo, 1980; Vvol. II, p 405.
(8) Murawski, L.; Chung, C. H.; Mackenzie, J. D. *J. Non-Cryst. Solids* **1972**, *32*, 91.
(9) Curry-Hyde, H. E.; Musch, H.; Baiker, A. *Appl. Catal.* **1990**, *65*, 211.
(10) Cao, H.; Suib, S. L. *J. Am. Chem. Soc.* **1994**, *116*, 5334.
(11) Ao, B.; Kummerl, L.; Haarer, D. *Adv. Mater.* **1995**, *7*, 495.
(12) Mallinson, J. C. *The Foundations of Magnetic Recording*; Academic: Berkeley, CA, 1987; Chapter 3.
(13) Bradley, F. N. *Materials for Magnetic Functions*; Hayden: New York, 1976; Chapter 2.
(14) Singhal, M.; Chhabra, P.; Kang, P.; Shah, D. O. *Mater. Res. Bull.* **1997**, *32*, 239.
(15) Brett, M. J.; Parsons, R. P. *Solid State Commun.* **1985**, 603.
(16) Mitsuyu, T.; Yamakazi, O.; Ohji, K.; Wasa, K. *Ferroelectrics* **1982**, *42*, 233.
(17) Jiang, Y.; Decker, S.; Mohs, C.; Klabunde, K. J. *J. Catal.* **1998**, *180*, 24.
(18) Dow, W. P.; Huang, T. J. *J. Catal.* **1996**, *160*, 171.
(19) Larsson, P. O.; Andersson, A.; Wallengerg, R. L. Svensson, B. *J. Catal* **1996**, *163*, 279.
(20) Sakohara, S.; Ishida, M.; Anderson, M. A. *J. Phys. Chem. B* **1998**, *102*, 10169.
(21) Maruyama, T.; Shionoya, J. *J. Mater. Sci. Lett.* **1992**, *11*, 170.
(22) Brookshier, M. A.; Chusuei, C. C.; Goodman, D. W. *Langmuir* **1999**, *15*, 2043.
(23) Muhammed, M. *Analusis* **1996**, *24*, M12.
(24) Verelst, M.; Snoeck, E.; Ely, T. O.; Lecante, P.; Amiens, C.; Roucau, C.; Mosset, A.; Chaudret, B. *Mater. Sci. Forum* **1998**, *269*, 403.
(25) Suslick, K. S., Ed. *Ultrasound: its Chemical, Physical and Biological Effects*; VCH: Weinheim, Germany, 1988.
(26) Suslick, K. S.; Choe, S. B.; Cichowals, A. A.; Grinstaff, M. W. *Nature* **1991**, *353*, 414.
(27) Dhas, N. A.; Gedanken, A. *Chem. Mater.* **1997**, *9*, 3159.
(28) Dhas, N. A.; Gedanken, A. *J. Phys. Chem.* **1997**, *101*, 9495.
(29) Patra, A.; Sominska, E.; Ramesh, S.; Koltypin, Yu.; Zhong, Z.; Minti, H.; Reisfeld, R.; Gedanken, A. *J. Phys. Chem. B* **1999**, *103*, 3361.
(30) Avivi, S.; Mastai, Y.; Hodes, G.; Gedanken, A. *J. Am. Chem. Soc.* **1999**, *121*, 4196.

10.1021/cm000166z CCC: $19.00
Published on Web 07/14/2000

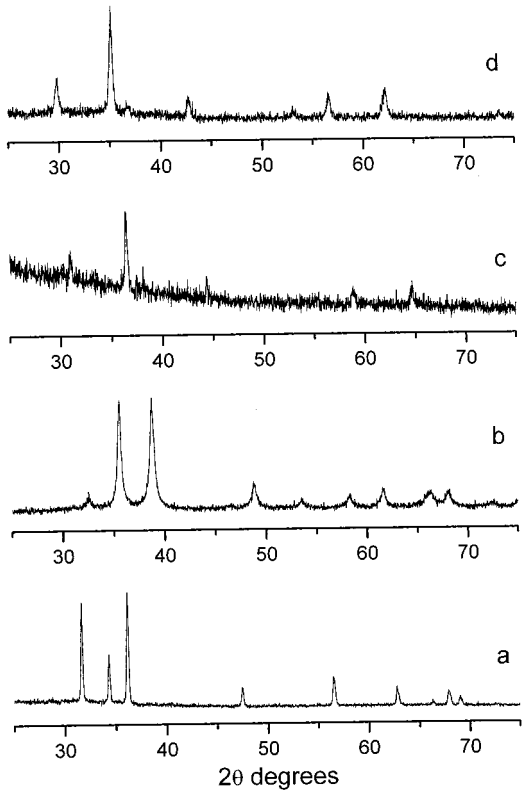

Figure 1. X-ray diffraction pattern of as-prepared metal oxide nanoparticles when water used as a solvent: (a) ZnO; (b) CuO; (c) Co_3O_4, (d) Fe_3O_4.

in 100 mL of doubly distilled deoxygenated water or 10% water−DMF is irradiated with a high-intensity ultrasonic horn (Ti-horn, 20 kHz, 100 W/cm^2) under 1.5 atm of argon at room temperature for 3 h. The product obtained is washed thoroughly with doubly distilled water and finally with absolute ethanol in an inert glovebox (O_2 < 1 ppm) and dried in a vacuum. The XRD measurements were carried out with a Bruker D8. Elemental analysis was carried out by an Eager 200 CHN analyzer. EDAX measurements were carried out on a JEOL JSM-840 scanning electron microscope. The transmission electron micrographs (TEM) were obtained by employing a JEOL-JEM 100SX microscope. Samples for the TEM examination were prepared by suspending dried samples in absolute ethanol. A drop of the sample suspension was allowed to dry on a copper grid (400 mesh, electron microscopy sciences) coated with a carbon film. Since the particles are heavily aggregated, the small separated particles detected in the TEM serve as our measure of the particle sizes. The surface area (BET) measurements were carried out using a Micromeritics-Gemini surface area analyzer, employing nitrogen gas adsorption. Diffuse reflection spectroscopy (DRS) measurements were carried out on a Varian Cary-500 spectrophotometer equipped with an integrated sphere. Spectra were recorded at room temperature, in the 1000−200 nm range, with a scanning speed of 100 nm/min. $MgCO_3$ was used as a reference.

Results

Figure 1 illustrates the XRD patterns of the as-prepared materials when water used as a solvent for (a) ZnO, (b) CuO, (c) Co_3O_4, and (d) Fe_3O_4. The XRD patterns match that of JCPDS cards Nos. (a) 36-1451, (b) 48-1548, (c) 42-1467, and (d) 19-0629, respectively. The particle size is calculated using the Debye−Scherer formula,[31] and the results are presented in Table 1. EDAX and C, H, and N analysis results showed that the resulting powder contains only metal, oxygen, and trace of carbon (estimated <2%) for all the metal oxides. Figure 2 illustrates the TEM images of the different as-prepared TM oxides made in water and 10% water−DMF as solvents. All the oxides are nanocrystalline, and the particle sizes measured from the TEM pictures of CuO, ZnO, Co_3O_4, and Fe_3O_4 are 20 nm (length (L)) and 2 nm (width (W)), (6), 340 nm (250), 30 nm (20), and 20 nm (8), respectively, when water (water−DMF) are used as solvents. The extent of agglomeration is minimal except in the case of CuO(water). The TEM picture of CuO(water) shows the agglomeration of needlelike particles, while for the water−DMF solution spherical particles are observed. Unlike the sonochemistry of TM carbonyls,[26,28] there is no sign of amorphous material from the TM oxides. The different particle sizes and morphology of metal oxide determine the surface area. The surface area results for the TM oxides are also presented in Table 1. The results show a dramatic increase in the surface area when the solvent is changed from water to 10% water−DMF. We observe higher yields of metal oxides when 10% water−DMF is used as a solvent.

We have measured the optical diffusion reflection spectra of the metal oxide powders in order to resolve the excitonic or interband (valence-conduction band) transitions of metal oxides, which allows us to calculate the band gap. The optical band gap E_g was estimated from the DRS spectra. The spectra shown in Figure 3 are given as plots of the Kubelka−Munck remission function[32,33] (converted from the diffuse reflection values by the spectrophotometer software) vs eV. These plots correspond fairly with absorption spectra. When water is used as a solvent we obtain E_g's = 2.18, 3.35, and 2.26 (3.40)[50] eV for CuO, ZnO, and Co_3O_4, respectively. When the solvent is changed from water to 10% water−DMF the estimated E_g's = 3.35 and 2.26 (3.40)[50] eV for ZnO and Co_3O_4, respectively. The results show that there is no appreciable difference in band gap energies when we change the solvent from water to 10% water−DMF, except in case of CuO, which is expected because the particle size difference is large. In other cases, this effect is not appreciable. These band gap energy values are compared to that of the bulk, as seen in Table 2. We observe a quantum size effect only for CuO and Co_3O_4. This can be explained because the particles sizes for these materials are below the Bohr diameter. For CuO, the E_g value obtained in water is 2.18 eV, while in 10% water−DMF it is difficult to determine the E_g from the DRS because of the very slow and shallow increase in the reflection. It seems as if a much higher E_g value is obtained for CuO, as compared to its bulk band gap. This can be attributed perhaps to the dramatic changes in the shape of the CuO particles. In the case of ZnO, this effect is not seen because size quantization effects are expected to be predominant when the particle size is less than 300 nm.[35] The multiple band gap for the Co_3O_4 particles indicates the possibility

(31) *X-ray Diffraction procedures*; Klug, H., Alexander, L., Eds.; Wiley: New York, 1962; p 125.
(32) Kubelka, D.; Munk, L. *J. Opt. Soc. Am.* **1948**, *38*, 448.
(33) Kortum, G. *Reflectance Spectroscopy*; Springer: Berlin, 1973.
(34) Santra, K.; Sarkar, C. K.; Mukherjee, M. K.; Gosh, B. *Thin Solid Films* **1992**, *213*, 226.
(35) Wong, E. M.; Searson, P. C. *Appl. Phys. Lett.* **1999**, *74*, 2939.

Table 1. BET Multipoint Surface Area and Particle Sizes from the Debye−Scherer Formula and TEM of the Different TM Oxide Nanoparticles Obtained from Water and 10% Water−DMF as Solvents

	water			10% water−DMF		
metal oxide	BET (m^2/g)	Debye−Scherer (nm)	TEM (nm)	BET (m^2/g)	Debye−Scherer (nm(	TEM (nm)
CuO	35		20 (L), 2 (W)	114	4	6
ZnO	10	310	340	14	240	250
Co_3O_4	135	25	30	156	15	20
Fe_3O_4	126	15	20	144	5	8

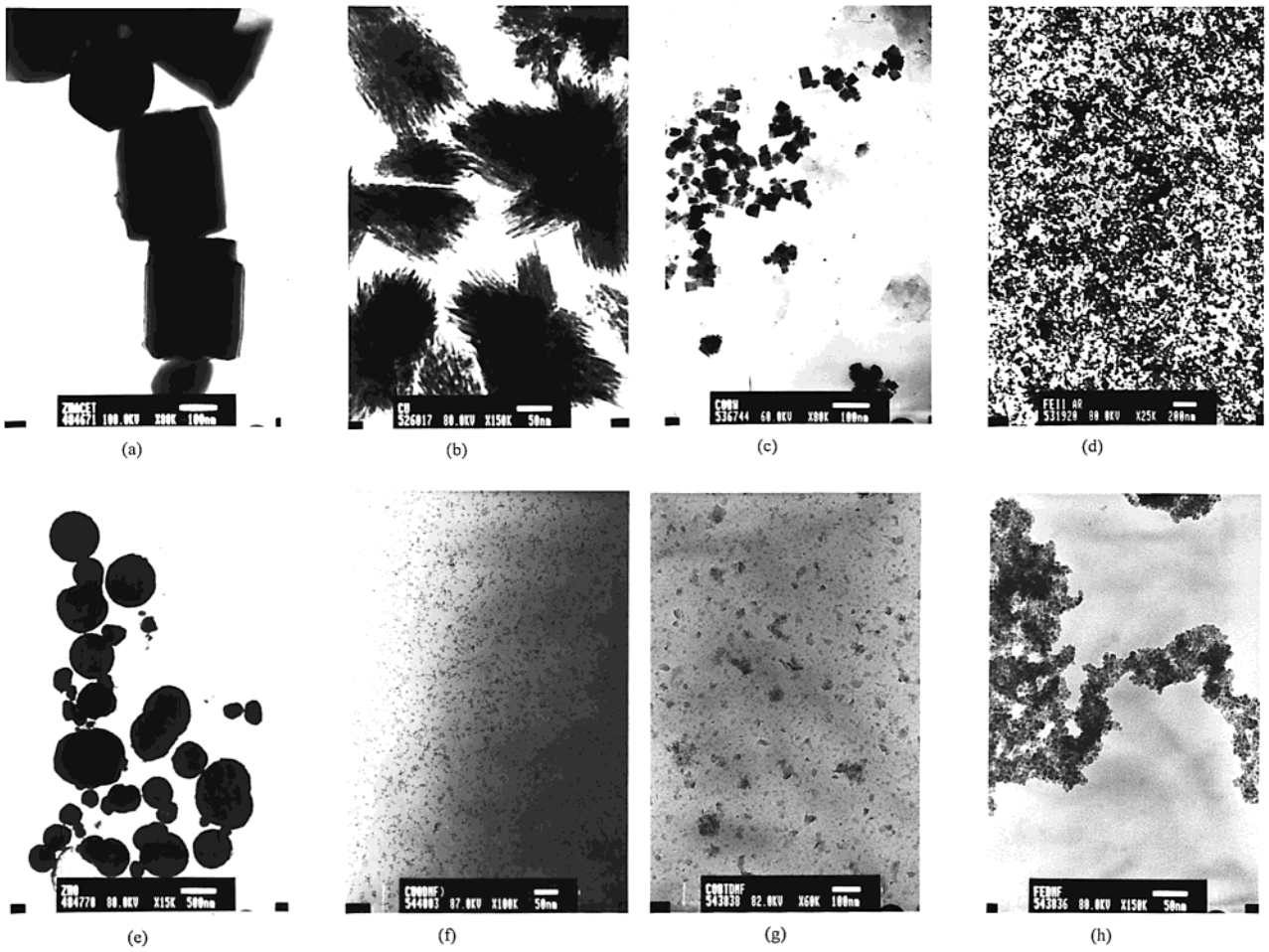

Figure 2. Transmission electron micrographs of the as-prepared metal oxide nanoparticles: (a) ZnO, (b) CuO, (c) Co_3O_4, (d) Fe_3O_4 (when water is used as a solvent), (e) ZnO, (f) CuO, (g) Co_3O_4, (h) Fe_3O_4 (when 10% water−DMF is used as a solvent).

of degeneracy of the valence band.[37] However it should be noted that the DRS has been reported to systematically underestimate the band gap with an error which increases with decreasing crystallite size.[33] For this reason, the band gap estimates are only approximate.

Discussion

Mechanism for the Sonochemical Formation of Fe_3O_4, Co_3O_4, CuO, and ZnO Nanoparticles. The chemical reactions reported to be driven by intense ultrasonic waves that are strong enough to produce cavitation are oxidation, reduction, dissolution, decomposition, and hydrolysis.[25,39−41] Other reactions, such as the promotion of polymerization, have also been reported to be induced by ultrasound. These reactions can occur in three different regions[42,43] surrounding the collapse of a bubble in aqueous media. They are the following: (a) the inner environment (gas phase) of the collapsing bubble, where elevated temperatures (several thousands of degrees) and high pressures (hundreds of atmospheres) are produced, causing the pyrolysis of water into H and OH radicals; (b) the interfacial liquid region between the cavitation bubbles and bulk solution.

(36) Shen Cheng, C.; Serizawa, M.; Sakata, H.; Hirayama, T. *Mater. Chem. Phy.* **1998**, *53*, 225.
(37) Murad, W. A.; Alshamari, S. M.; Alkhateb, F. H.; Misho, R. H. *Phys. Status Solidi A* **1998**, *106*, K143.
(38) Alegria, A. E.; Lion, Y.; Kondo, T.; Riesz, P. *J. Phys. Chem.* **1989**, *93*, 3, 4908.
(39) Gutierrez, M.; Henglein, A. *J. Phys. Chem.* **1988**, *92*, 2978.
(40) Sostaric, J. Z.; Mulvaney, P.; Grieser, F. *J. Chem. Soc., Faraday Trans.* **1995**, *91*, 2843.
(41) Gutierrez, M.; Henglein, A.; Dohrmann, J. *J. Phys. Chem.* **1987**, *91*, 6687.
(42) (a) Suslick, K. S.; Hammerton, D. A. *IEEE Trans. Sonics Ultrason.* **1986**, SU-33, 143. (b) Suslick, K. S.; Hammerton, D. A. *Ultrason. Int.* **1985**, 231. (c) Suslick, K. S.; Cline, R. E.; Hammerton, D. A. *Ultrason. Symp. Proc.* **1985**, *2*, 1116.
(43) (a) Mason, T. J., Ed. *Advances in Sonochemistry*; JAI Press: London, 1990; Vol. 1. (b) Mason, T. J., Ed. *Advances in Sonochemistry*; JAI Press: London, 1991; Vol. 2. (c) Mason, T. J., Ed. *Advances in Sonochemistry*; JAI Press: London, 1993; Vol. 3.

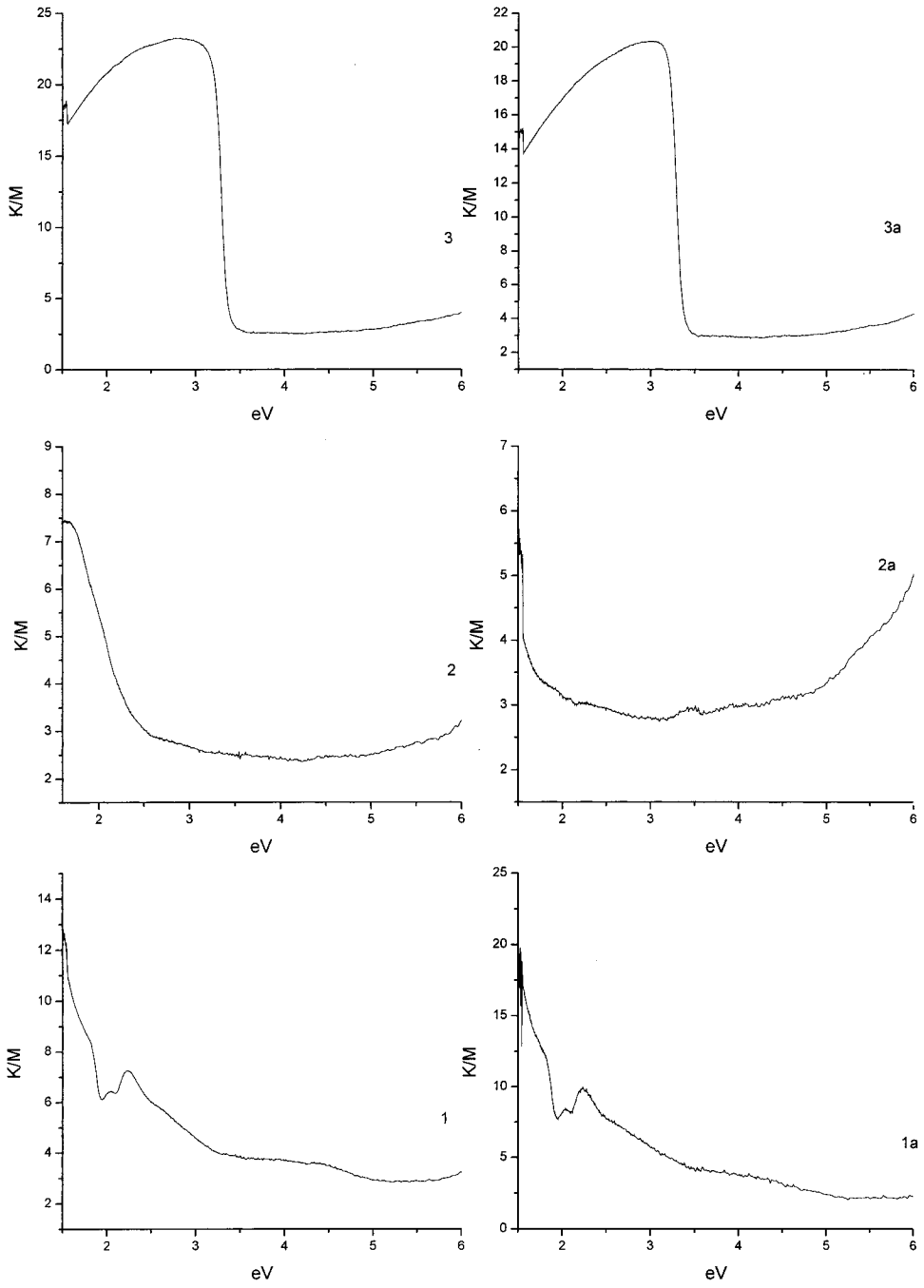

Figure 3. Kubelka−Munch remission function versus eV of metal oxide nanoparticles: (1) Co_3O_4, (2) CuO, (3) ZnO (when water is used as solvent); (1a) Co_3O_4, (2a) CuO, (3a) ZnO (when 10% water−DMF is used as a solvent).

Table 2. Experimental and Literature Band Gap Energies (E_g) of Different Metal Oxide Nanoparticles Obtained from Water as Solvent

metal oxide	bulk (eV)	exptl (eV)
CuO	1.85[34]	2.18
ZnO	3.35[35]	3.35
Co_3O_4	1.50−1.52, 1.88−1.95[36]	2.26, 3.4

The temperature in this region is lower than that of the interior of the bubbles and the reaction is a liquid-phase reaction; however the temperature is still high enough to rupture chemical bonds. In addition, greater local hydroxyl radical concentrations in this region have been reported.[44] The third region (c) is the bulk of the solution, which is at ambient temperatures and where the reaction between reactant molecules and surviving OH or H can still take place. In our case, among the above-mentioned three regions, it appears that the sonochemical reaction occurs within the interfacial region. This is because the metal acetates are ionic and due to their low vapor pressure their vapors will not exist in region a. We propose two types of mechanisms for the formation of the metal oxides from aqueous metal acetates: sonochemical oxidation for the formation of Fe_3O_4 and Co_3O_4 and sonochemical hydrolysis for the formation of CuO and ZnO. The pH values of the reaction mixtures were measured before and after sonication and the results are presented in Table 3. Since the pH of pure DMF is ∼9.6, the pH values

(44) Gutierrez, M.; Henglein, A.; Ibanez, F. *J. Phys. Chem.* **1995**, *95*, 5, 6044.

Table 3. Yields of Metal Oxides and pH Measurements of the Reaction Mixtures before Sonication (BS) and after Sonication (AS)

	water			10% water−DMF		
metal oxide	BS	AS	yield (%)	BS	AS	yield (%)
ZnO	5.9	5.2	10	9.2	8.2	30
CuO	5.7	4.9	22	9.0	8.1	35
Co_3O_4	5.2	5.7	8	9.1	9.6	15
Fe_3O_4	5.3	5.9	25	8.9	9.4	32

obtained for water−DMF solutions are higher than those measured for the water solutions. The results indicated that during the sonication H^+ ions are generated in the formation of CuO and ZnO and OH^- ions are formed in the fabrication of Fe_3O_4 and Co_3O_4.

(a) Sonochemical Oxidation. The mechanism of the formation of Fe_3O_4 and Co_3O_4 nanoparticles takes into consideration the radical species generated from the water molecules which decompose in region a. The likely reaction steps and explanation for the sonochemical oxidation process can be summarized as follows:

$$H_2O \text{))))) } H^\bullet + OH^\bullet \quad (1)$$

$$H^\bullet + H^\bullet \rightarrow H_2 \quad (2)$$

$$OH^\bullet + OH^\bullet \rightarrow H_2O_2 \quad (3)$$

$$Fe(CH_3COO)_2(s) \rightarrow Fe^{2+}(aq) + 2(CH_3COO)^-(aq)$$

or

$$Co(CH_3COO)_2(s) \rightarrow Co^{2+}(aq) + 2(CH_3COO)^-(aq)$$

The oxidant H_2O_2 thus generated can initiate the oxidation of Fe(II) or Co(II):

$$2Fe(II) + H_2O_2 \rightarrow 2Fe(III) + 2OH^- \quad (4)$$

or

$$2Co(II) + H_2O_2 \rightarrow 2Co(III) + 2OH^-$$

(b) Sonochemical Hydrolysis. The likely reaction steps and possible explanation for sonohydrolysis are as follows:

$$Cu^{2+}(aq) + H_2O(l) \rightarrow Cu(O)(s) + 2H^+(aq)$$

or

$$Zn^{2+}(aq) + H_2O(l) \rightarrow Zn(O)(s) + 2H^+(aq)$$

Copper and zinc oxides nanoparticles are formed through the sonohydrolysis mechanism. Similar ideas have been formulated by Henglein and co-workers[46] by studying the sonolysis of a nonvolatile solute, such as acetate anion, as in our case. The formation of CuO and ZnO also occurs at the interface of the solution bubble.

Numerous factors influence the acoustic cavitation and sonochemical yields.[48] In the bulk solution, factors favoring maximum acoustic cavitation and sonochemical yields are (i) low viscosity, (ii) high surface tension, (iii) low vapor pressure, and (iv) high sound speed. DMF is freely miscible with water, and DMF fulfills all of the above-mentioned criteria. We have carried out the reactions in 10% water−DMF solution, where we observe better yields than with water alone, which is expected. The increased availability of DMF molecules both for pyrolysis and for hydrogen abstraction reactions at a higher mole fraction of DMF and low vapor pressure of DMF (3.7 Torr at 25 °C, compared to water and 24 Torr at 25 °C) are the most likely factors responsible for the continuing increase of the sonochemical radical yields at high DMF concentrations. The DMF accumulated at the interfacial region[49] is likely to outcompete the concurrent process of •OH removal. While the reaction with •OH radicals may be dominant pathways for the production of $^\bullet CH_2N(CH_3)CHO$ radicals at low DMF concentrations, at a high mole fraction of DMF, hydrogen abstraction by the methyl radical predominates.[49] Sonochemical oxidation is enhanced in case of 10% water−DMF as a solvent.

We observe higher yields for 10% water−DMF as a solvent in the case of sonohydrolysis as well. The temperature generated during the collapse of a gas-filled cavity is higher in the case of low vapor pressure solvents.[42] Hence the temperature at the interfacial region of interest is also higher in the 10% water−DMF than in pure water. As mentioned above, the DMF vapor pressure as well as 10% water−DMF is lower than that of water.

Conclusions

Transition metal oxides have been prepared from metal acetates by the sonochemical method. When the solvent is changed from water to 10% water−DMF, different sizes, morphologies, and yields are obtained for the transition metal oxides. This method can be extended to other transition metal acetates in order to obtain metal oxides.

Acknowledgment. R.V.K. thanks the Bar-Ilan Research Authority for his postdoctoral fellowship. A.G. thanks the German Ministry of Science through the Deutche-Israeli Program, DIP, for its support and gratefully acknowledges receipt of a NEDO International Joint Research Grant. The authors are grateful to Prof. M. Deutsch, Department of Physics, Prof. Z. Malik, Department of Life Sciences, and Dr. A. Zaban, Department of Chemistry, for extending their facilities to us. We also thank Dr. Shifra Hochberg for editorial assistance.

CM000166Z

(45) Mizukoshi, M.; Oshima, R.; Maeda, Y.; Nagata, Y. *Langmuir* **1999**, *15*, 2733.
(46) Gutierrez, M.; Henglein, A.; Fisher, Ch. H. *Int. J. Radiat. Biol.* **1986**, *50*, 313.
(47) Riesz, P.; Kondo, T.; Carmichael, A. J. *Free Radical Res. Commun.* **1993**, *19*, S45.
(48) Flynn, H. G. In *Physical Acoustics: Principles and Methods*; Mason, W. P., Ed.; Academic Press: New York, 1964; p 165.
(49) Misik, V.; Kirschenbaum, L. J.; Riesz, P. *J. Phys. Chem.* **1995**, *99*, 5970.
(50) The number in parentheses (3.4) is due to the multiple band gap detected for Co_3O_4. This double band gap is also observed in ref 37.